Supplementary material to "Computing Lagrangian means"

Kafiabad & Vanneste

Numerical analysis of Lagrangian averaging in 2D flow

In this supplementary document, we present further numerical analysis of Lagrangian averaging for the 2D incompressible inviscid example of section 4.1. We expressed in this section that "three numerical solutions for $\tilde{\zeta}^{\mathrm{L}}$ converge to each other and to ζ as the spatial resolution increases or the length of the averaging interval decreases". Figures 1, 2 and 3 below show that increasing the spatial resolution reduces the error in different approaches and all the solutions converge to each other. In these figures, we added a row that shows the error values defined as $|\tilde{\zeta}^L - \zeta|/\max(|\zeta|)$. In other words, the panels (f), (g) and (h) are the normalised differences of (b), (c) and (d) with the panel (a), respectively.

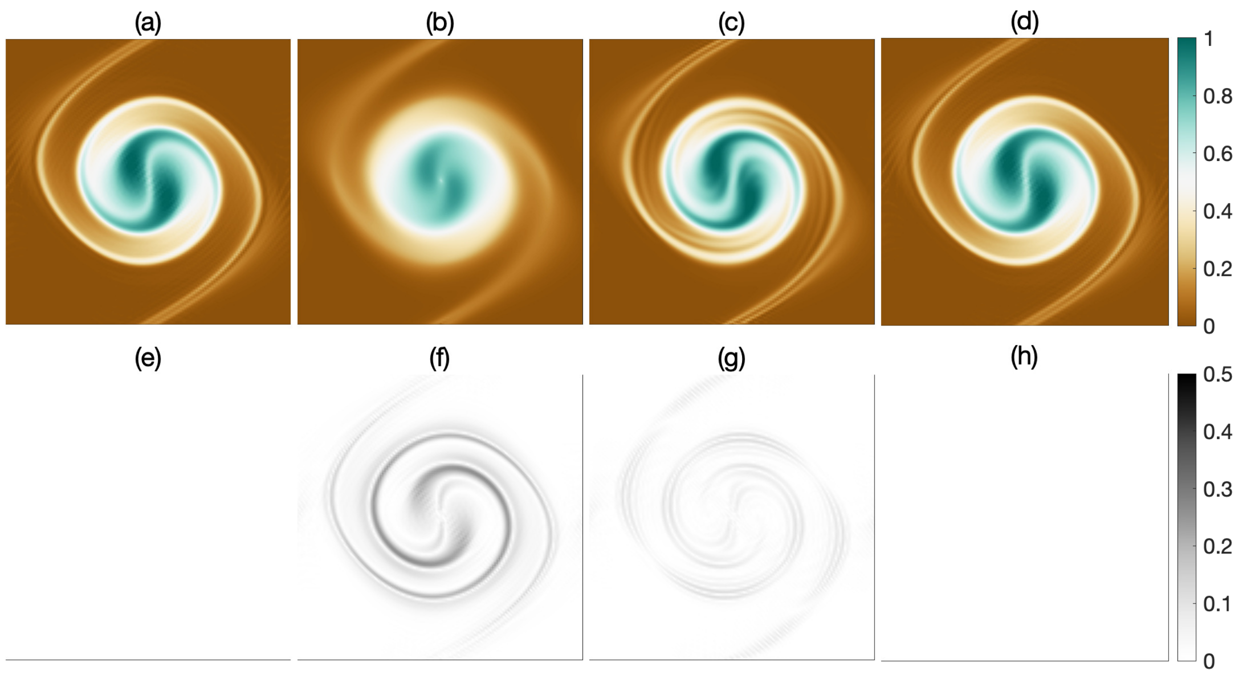

Figure 1: Top row is Figure 4 of the paper. The added bottom row displays the error values defined as $|\tilde{\zeta}^L - \zeta|/\max(|\zeta|)$.

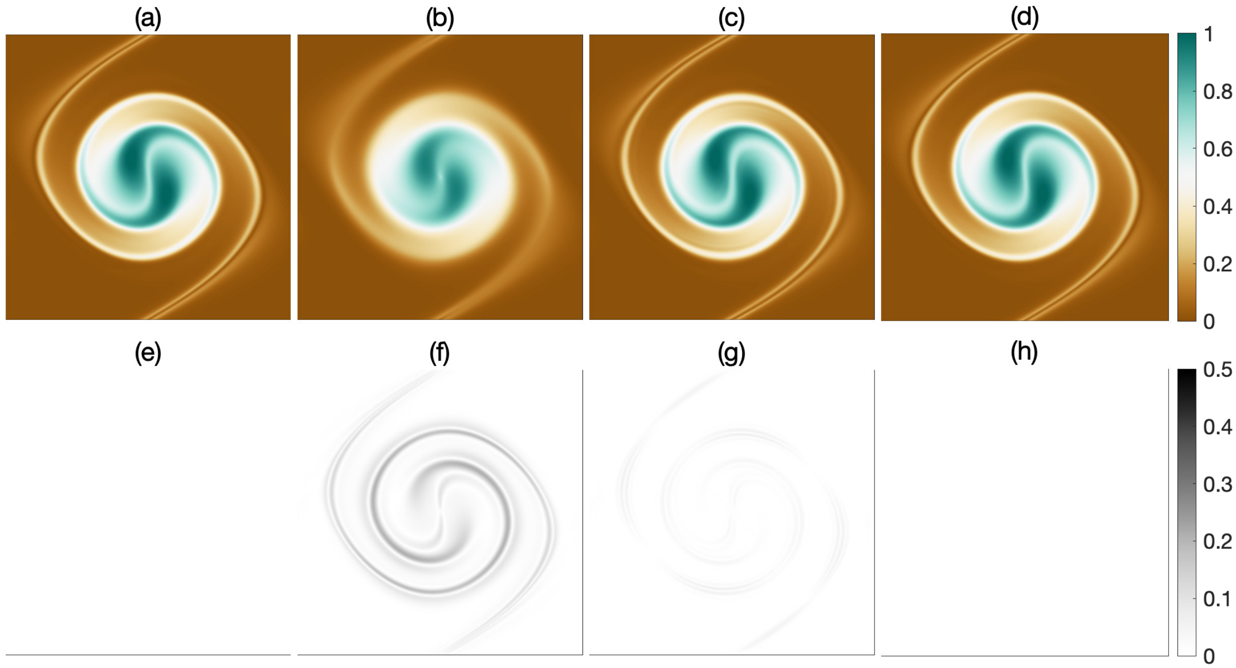

Figure 2: Same as figure 1 but for increased resolution of 256^2

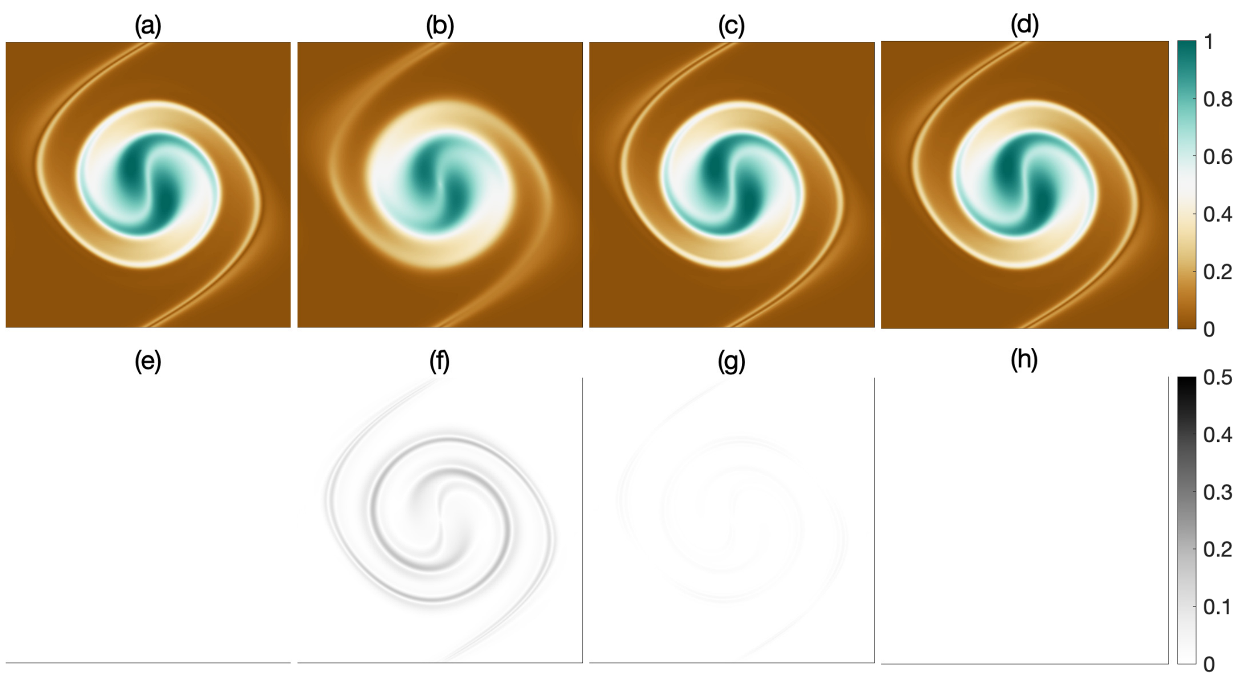

Figure 3: Same as figure 1 but for increased document of 384^2.

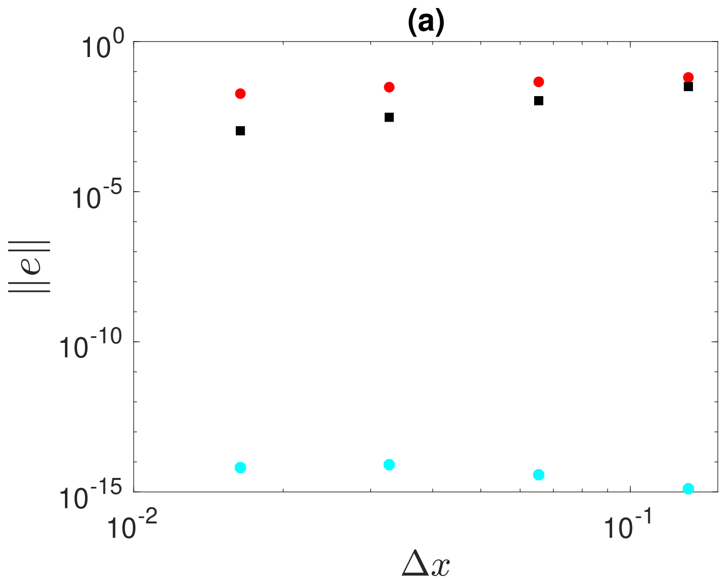

Figure 4: Numerical error as a function of grid spacing for semi-Lagrangian discretisation with linear interpolation (red dots), semi-Lagrangian discretisation with cubic interpolation (black square), and pseudospectral (cyan stars) methods. The instantaneous vorticity at the corresponding resolution is used as the 'truth'.

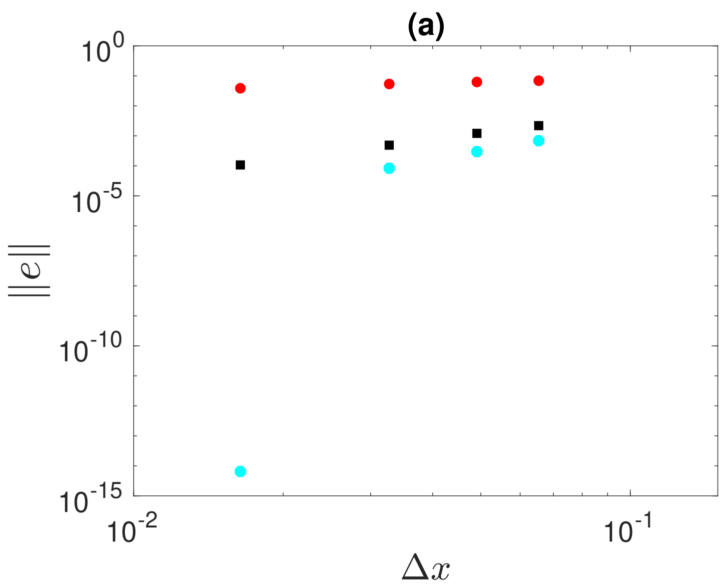

Figure 5: Numerical error as a function of grid spacing for semi-Lagrangian discretisation with linear interpolation (red dots), semi-Lagrangian discretisation with cubic interpolation (black square), and pseudospectral (cyan stars) methods. The 'truth' is taken as the instantaneous vorticity obtained from the highest resolution pseudospectral simulation, which is decimated for lower resolutions.

Figure 4 shows the following error norm for different approaches of computing Lagrangian mean at different spatial resolutions

$$\|e\| = \sqrt{\frac{1}{N_x N_y}\sum_i (|\tilde{\zeta}^L - \zeta_{\mathrm{truth}}|)^2}, \tag{1}$$

where the summation is carried out over all spatial grid point, and N_x and N_y are the number of grid points in each dimension. The instantaneous vorticity at the **corresponding** resolution is used as the 'truth' or 'exact' value. We should stress that the example in section 4.1 is very special (the Lagrangian mean vorticity in the sense of $\tilde{\zeta}^{\mathrm{L}}$ is the same as the instantaneous vorticity) and is used just as a check point for the implementation of strategy 1. In particular, for this example, it can be shown that when the dynamical equation for the vorticity and the Lagrangian mean PDEs are solved pseudospectrally at the same resolution, the difference between instantaneous and Lagrangian mean vorticity is down to round-off error (the equations become practically the same). This can be seen in figure 4. We tried a different scenario where the 'truth' is taken as the instantaneous vorticity obtained from the highest resolution pseudospectral simulation. We then computed Lagrangian mean off-line using the decimated fields of this high-resolution simulation. The results are depicted in figure 5 below. The error in both figures is calculated as the RMS of the difference between the computed Lagrangian and the 'truth'. These plots confirm the validity of our implementation.

Figures 6 and 7 shows that different approaches for computing Lagrangian mean converge to one another by lowering the averaging intervals.

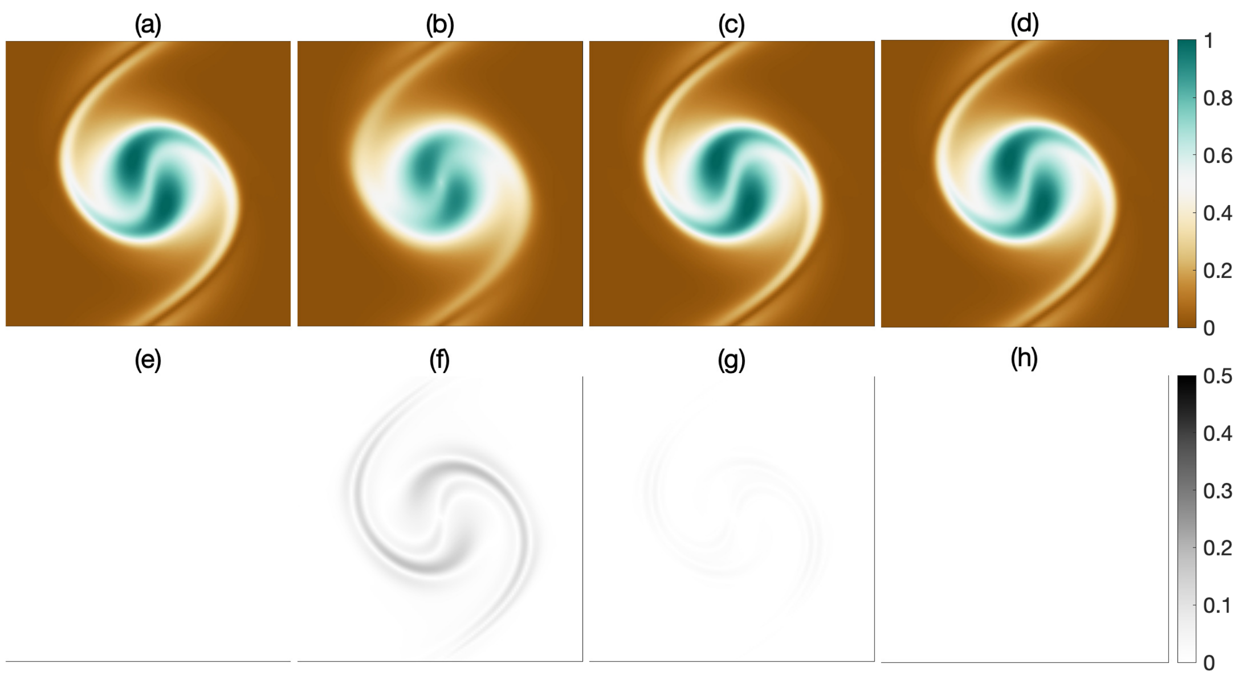

Figure 6: Same as figure 1 but for averaging interval of $T = 15$

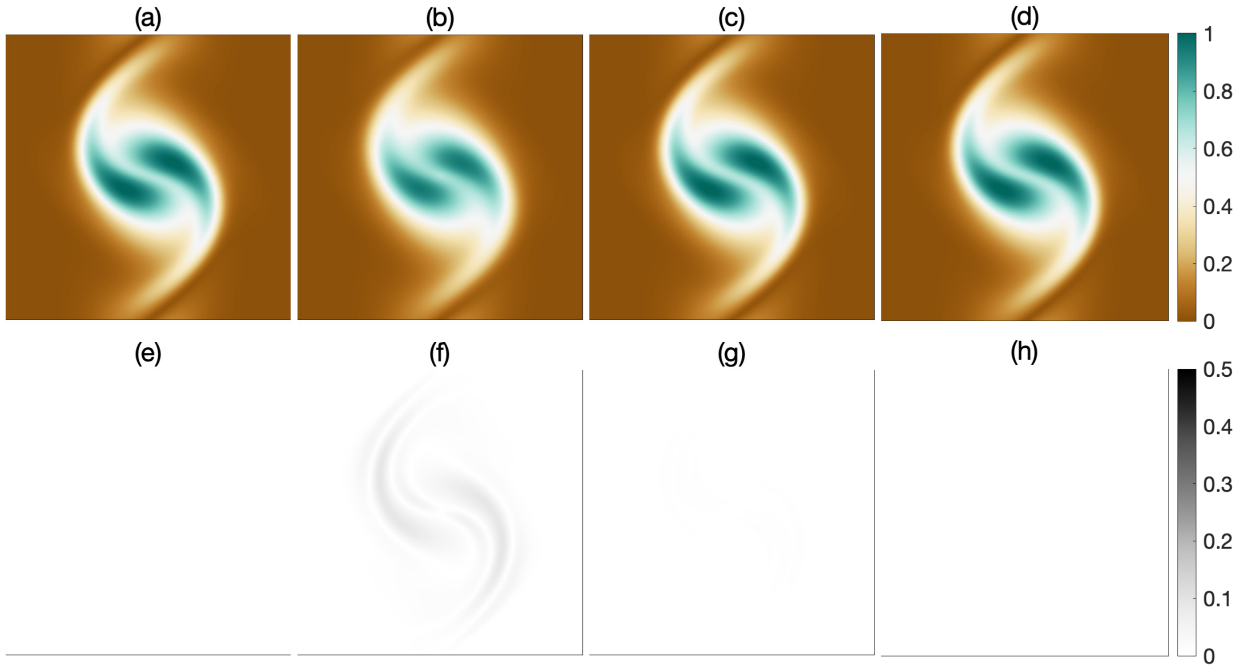

Figure 7: Same as figure 1 but for averaging interval of $T = 10$